Journal of Photochemistry and Photobiology A: Chemistry 217 (2011) 341–346

Contents lists available at ScienceDirect

Journal of Photochemistry and Photobiology A: Chemistry

journal homepage: www.elsevier.com/locate/jphotochem

Photoisomerization in an analogous set of ruthenium sulfoxide complexes

Brianne L. Porter[a], Beth Anne McClure[a], Eric R. Abrams[a], James T. Engle[b], Christopher J. Ziegler[b], Jeffrey J. Rack[a,*]

[a] Department of Chemistry and Biochemistry, Nanoscale and Quantum Phenomena Institute, Ohio University, Athens, OH 45701, USA
[b] Department of Chemistry, Knight Chemical Laboratory, University of Akron, Akron, OH 44325, USA

ARTICLE INFO

Article history:
Received 23 June 2010
Received in revised form 2 November 2010
Accepted 7 November 2010
Available online 13 November 2010

Keywords:
Photochromic
Ruthenium
Polypyridine
Isomerization

ABSTRACT

Complexes of the type $[Ru(bpy)_2(OSOBnR)](PF_6)$ where bpy is 2,2′-bipyridine and OSOBnR is a 4-substituted benzylsulfinylbenzoate with R = NO_2, F, Cl, H, CH_3, CF_3 and OCH_3, have been prepared and investigated by ^{1}H NMR spectroscopy, cyclic voltammetry and UV–vis spectroscopy. Despite the distance of the R group from ruthenium, the $Ru^{3+/2+}$ reduction potential and charge transfer absorption maximum vary predictably with the electron withdrawing nature of the group.

1. Introduction

Electron transfer induced conformational changes are central to the operation of molecular machines and other types of molecular bistability [1–3]. A number of studies have revealed that reduction or oxidation of interlocked rotaxanes results in translocation of a molecular unit from one site to another [4–6]. However, certain transition metal complexes exhibit bistability through isomerization of bound ambidentate ligands [7–12]. For example, pentaammine ruthenium complexes of dimethylsulfoxide (DMSO) undergo intramolecular linkage isomerization (S vs. O) following oxidation and reduction of ruthenium [13–16]. We have developed a class of simultaneously photochromic and electrochromic polypyridine ruthenium sulfoxide complexes based on S → O and O → S isomerization [17–26]. In our study of these complexes, we have found that changes to a substituent R group affects the S-bonded $Ru^{3+/2+}$ reduction potential, the S-bonded charge-transfer absorption maximum and the S → O isomerization quantum yield. Interestingly, the corresponding O-bonded properties show no correlation with the identity of the R group.

2. Experimental

2.1. Materials

The reagents $RuCl_3{\cdot}xH_2O$ and silver hexafluorophosphate ($AgPF_6$) were purchased from Strem. The reagents 2,2′-bipyridine (bpy), thiosalicylic acid, *m*-chloroperoxybenzoic acid, triethylamine, 4-trifluoromethylbenzyl bromide, 4-fluorobenzyl bromide, benzyl bromide, 4-methylbenzyl bromide, 4-chlorobenzyl bromide, 4-methoxybenzyl bromide, and 4-nitrobenzyl bromide were purchased from Aldrich and used as received. The compounds *cis*-$[Ru(bpy)_2Cl_2]{\cdot}2H_2O$ and $[Ru(bpy)_2(OSO\text{-}Bn)](PF_6)$ were synthesized according to published methods [27,28]. The solvents acetone, methanol, ethanol, diethyl ether, and dichloromethane were purchased from VWR and used without further purification. Tetrabutylammonium hexafluorophosphate ($TBAPF_6$) was purchased from Aldrich and recrystallized three times from ethanol. Acetonitrile for electrochemical experiments was HPLC grade and purchased from Burdick and Jackson and used without further purification. The synthesis and isolation of all ruthenium sulfoxide complexes were carried out in the dark or under red light conditions.

2.2. Instrumentation

Electronic absorption spectra were collected on an Agilent 8453 spectrophotometer. Bulk photolysis experiments were conducted using a 75 W Xenon-arc lamp (Oriel) fitted with a Canon standard camera UV filter. Proton nuclear magnetic resonance (^{1}H

* Corresponding author. Te.: +1 740-593-9702.
E-mail addresses: bp293206@ohio.edu (B.L. Porter), bm692806@ohio.edu (B.A. McClure), ea266105@ohio.edu (E.R. Abrams), jte3@uakron.edu (J.T. Engle), ziegler@uakron.edu (C.J. Ziegler), rackj@ohio.edu, rack@helios.phy.ohiou.edu (J.J. Rack).

1010-6030/$ – see front matter © 2010 Elsevier B.V. All rights reserved.
doi:10.1016/j.jphotochem.2010.11.002

NMR) spectra were collected in deuterated acetone (d^6-acetone) on either a 300 MHz Bruker spectrometer or a 500 MHz Varian INOVA500 spectrometer. Cyclic voltammetry was performed on a CH Instruments CHI 730A Electrochemical Analyzer. This workstation contains a digital simulation package as part of the software package to operate the workstation (CHI version 2.06). The working electrode was a Pt disk (Cypress Systems) electrode (1 mm). The counter and reference electrodes were Pt wire and Ag/Ag^+, respectively. Electrochemical measurements were performed in acetonitrile solutions containing 0.1 M $TBAPF_6$ electrolyte in a one compartment cell.

2.3. Quantum yield measurements

Quantum yield of isomerization measurements were determined by irradiating solutions of the complexes $[Ru(bpy)_2(OSO\text{-}BnR)]^+$ in methanol at room temperature. Photolysis was achieved using a PTI C-60 fluorimeter at the lower energy isosbestic point between S-bonded and O-bonded isomers. Incident radiation intensity, I_o, was determined using potassium ferrioxalate actinometry. Quantum yields of isomerization were calculated according to Eq. (1) [29] in which $d[O]/dt$ is the slope of the O-bonded concentration, [O] as a function of time for less than 10% converted to O-bonded, A_λ is the absorbance at the isosbestic point (λ) and V is the volume of irradiated solution (3 mL). The concentration of O-bonded isomer was determined using multi-linear regression:

$$\Phi_{s\to o} = \frac{(d[O]/dt)}{(I_o/V)(1-10^{-A\lambda})} \quad (1)$$

2.4. Crystallography

Crystals suitable for structural determination were obtained by slow evaporation of a concentrated methanol solution. Single crystal X-ray diffraction data were collected at 100 K (Bruker KRYOFLEX) on a Bruker SMART APEX CCD-based X-ray diffractometer system equipped with a Mo-target X-ray tube (λ = 0.71073 Å). The detector was placed at a distance of 5.009 cm from the crystal. Crystals were placed in paratone oil upon removal from the mother liquor and mounted on a plastic loop in the oil. Integration and refinement of crystal data were done using Bruker SAINT software package and Bruker SHELXTL (version 6.1) software package, respectively [30]. Absorption correction was completed by using the SADABS program.

2.5. Synthesis of ruthenium complexes

2-(4-Methyl-benzylsulfanyl)-benzoic acid, $OSBnCH_3$ (1). The compound thiosalicylic acid (598 mg, 3.88 mmol) was dissolved in 75 mL of methanol. Sodium hydroxide (330 mg, 8.25 mmol) was added in excess to the solution. The solution was stirred at 25 °C for 30 min. The solvent was removed by rotary evaporation. The remaining white precipitate was dissolved in 75 mL acetone. The compound 4-methylbenzyl bromide (800 mg, 4.32 mmol) was added to the solution. The solution was refluxed for approximately 4 h. The white precipitate was isolated by vacuum filtration and rinsed with diethyl ether. The precipitate was air dried for 1 h. The precipitate was dissolved in 35 mL of methanol. Concentrated HCl was added dropwise (approximately 20 mL) until the product precipitated as a white solid. The solid was isolated by vacuum filtration and rinsed with water and air dried. Yield: 903 mg (91%). ^{1}H NMR (d^6-acetone, 300 MHz) δ: 8.00 (d, 1 H), 7.49 (m, 2 H), 7.35 d, 2 H), 7.22 (t, 1 H), 7.15 (d, 2 H), 4.18 (s, 2 H), 2.29 (s, 3 H).

2-(4-Methyl-benzylsulfinyl)-benzoic acid, $OSOBnCH_3$ (2). The ligand $OS\text{-}BnCH_3$ (397 mg, 1.55 mmol) was dissolved in 60 mL of acetone. In another 20 mL of acetone 1 equivalent of *m*-chloroperoxybenzoic acid (453 mg 60% peroxo reagent by ^{1}H NMR, 1.58 mmol) was dissolved. The solution of *m*-chloroperoxybenzoic acid was added dropwise to the solution of $OS\text{-}BnCH_3$ over a period of 5 min. The solution was stirred at 25 °C for approximately 15 min. The acetone was removed by rotary evaporation. A minimum amount of diethyl ether was added to the residue and a white precipitate was isolated via vacuum filtration and air dried. Yield: 333 mg (79%). ^{1}H NMR (d^6-acetone, 300 MHz) δ: 8.19 (d, 1 H), 7.91 (d, 1 H), 7.74 (t, 1 H), 7.63 (t, 1 H), 7.10 (m, 4 H), 4.43 (d, 1 H), 3.75 (d, 1 H), 2.30 (s, 3 H).

$[Ru(bpy)_2(OSOBnCH_3)](PF_6)\cdot 1.8H_2O$ (3). This procedure and purification are done in the dark or under red light. The dark purple complex $[Ru(bpy)_2Cl_2]\cdot 2H_2O$ (212 mg, 0.408 mmol) was dissolved in 50 mL of ethanol with $OSO\text{-}BnCH_3$ (124 mg, 0.455 mmol), 2 equivalents of silver hexafluorophosphate ($AgPF_6$) (219 mg, 0.852 mmol) and excess triethylamine (150 μL). The solution was brought to reflux under nitrogen gas for approximately 4 h. The solution was cooled to −30 °C overnight to allow maximum precipitation of the AgCl. The AgCl was isolated by vacuum filtration and rinsed with ethanol and dichloromethane until filtrate was colorless. The solvent was removed by rotary evaporation. In order to remove the byproduct NEt_3HPF_6, the oily residue was dissolved in dichloromethane and extracted with an aqueous solution of $LiOH\cdot H_2O$ (~25 mg in 10 mL). The dichloromethane layer was dried with anhydrous magnesium sulfate and the solvent was removed by rotary evaporation. A minimal amount of methanol was added to the resulting residue. Approximately 5 mL of diethyl ether was added to the concentrated solution to precipitate the product. The solution was cooled to −30 °C for 15 min for complete precipitation. The product was isolated by vacuum filtration and air dried. Yield: 277 mg (82%). UV–vis (MeOH) $\lambda_{max}(\varepsilon)$ = 399 nm (7400) S-bonded, 349 nm (9400) and 496 nm (9400) O-bonded. $E^{\circ\prime}$ $Ru^{3+/2+}$ vs. Ag/Ag^+ = 0.89 V S-bonded, 0.52 V O-bonded. ^{1}H NMR (d^6-acetone, 500 MHz) δ: 9.50 (d, 1 H), 9.05 (d, 1 H), 8.90 (d, 1 H), 8.69 (m, 3 H), 8.52 (t, 1 H), 8.21 (t, 1 H), 8.10 (m, 3 H), 8.05 (t, 1 H), 7.90 (d, 1 H), 7.60 (m, 2 H), 7.45 (m, 5 H), 6.90 (d, 2 H), 6.60 (d, 2 H) 4.25 (d, 1 H), 3.94 (d, 1 H), 2.22 (s, 3 H). Elemental Analysis: Calculated for $[Ru(C_{10}H_8N_2)_2(C_{15}H_{13}O_3S)]PF_6\cdot 1.8H_2O$: Calculated: C: 48.64%, H: 3.81%, N: 6.48%. Found: C: 48.27%, H: 3.41%, N: 6.76%.

2.6. Synthesis of $[Ru(bpy_2)(OSO\text{-}BnCF_3)](PF_6)\cdot 1.3H_2O$

2-(4-Trifluoromethyl-benzylsulfanyl)-benzoic acid, $OSBnCF_3$ (4). 4 was prepared following the procedure as described above for complex 1 using 300 mg thiosalicylic acid and 520 mg of 4-trifluoromethylbenzyl bromide. Yield: 220 mg (54%). ^{1}H NMR (d^6-acetone, 300 MHz) δ: 8.02 (d, 1 H), 7.70 (dd, 4 H), 7.51 (m, 2 H), 7.25 (t, 1 H), 4.35 (s, 2 H).

2-(4-Trifluoromethyl-benzylsulfinyl)-benzoic acid, $OSOBnCF_3$ (5). 5 was prepared following the procedure as described above for complex 2 starting with 184 mg of 4. Yield: 147 mg (76%). ^{1}H NMR (d^6-acetone, 300 MHz) δ: 8.18 (d, 1 H), 7.80 (d, 1 H), 7.59–7.74 (m, 4 H), 7.37 (d, 2 H), 4.55 (d, 1 H), 4.02 (d, 1 H).

$[Ru(bpy_2)(OSOBnCF_3)](PF_6)\cdot 1.3H_2O$ (6). 6 was prepared following the procedure as described above for complex 3 starting with 76 mg $[Ru(bpy)_2Cl_2]\cdot 2H_2O$ and 64 mg of 5. Yield: 102 mg (77%). UV–vis (MeOH) $\lambda_{max}(\varepsilon)$ = 392 nm (7100) S-bonded, 350 nm (9200) and 496 nm (9300) O-bonded. $E^{\circ\prime}$ $Ru^{3+/2+}$ vs. Ag/Ag^+ = 0.93 V S-bonded, 0.53 V O-bonded. ^{1}H NMR (d^6-acetone, 500 MHz) δ: 9.54 (d, 1 H), 8.99 (d, 1 H), 8.87 (d, 1 H), 8.68 (m, 3 H), 8.53 (t, 1 H), 8.26 (t, 1 H), 8.16 (m, 3 H), 8.10 (t, 1 H), 7.93 (d, 1 H), 7.58 (m, 2 H), 7.52 (t, 2 H), 7.46 (t, 1 H), 7.38 (m, 3 H), 7.29 (d, 1 H), 6.88 (d, 2 H), 4.46 (d, 1 H), 4.18 (d, 1 H). Elemental Analysis: Calculated for $[Ru(C_{10}H_8N_2)_2(C_{15}H_{10}O_3F_3S)]PF_6\cdot 1.3H_2O$: Calculated: C: 46.23%, H: 3.18%, O: 7.57%, N: 6.16%, S: 3.53%. Found: C: 45.92%, H: 3.13%, O: 7.59%, N: 6.44%, S: 3.30%.

2.7. Synthesis of [Ru(bpy)$_2$(OSO-BnCl)](PF$_6$)·0.75H$_2$O

2-(4-Chloro-benzylsulfanyl)-benzoic acid, OSBnCl (7). 7 was prepared following the procedure as described above for complex 1 using 400 mg thiosalicylic acid and 586 mg of 4-chlorobenzyl bromide. Yield: 509 mg (70%). ^{1}H NMR (d^6-acetone, 300 MHz) δ: 8.00 (d, 1 H), 7.49 (m, 4 H), 7.37 (d, 2 H), 7.24 (m, 1 H), 4.23 (s, 2 H).

2-(4-Chloro-benzylsulfinyl)-benzoic acid, OSOBnCl (8). 8 was prepared following the procedure as described above for complex 2 starting with complex 345 mg of 7. Yield: 313 mg (85%). ^{1}H NMR (d^6-acetone, 300 MHz) δ: 8.19 (d, 1 H), 7.80 (d, 1 H), 7.68 (t, 1 H), 7.59 (t, 1 H), 7.29 (d, 2 H), 7.17 (d, 2 H), 4.45 (d, 1 H), 3.90 (d, 1 H).

[Ru(bpy)$_2$(OSOBnCl)](PF$_6$)·0.75H$_2$O (9). 9 was prepared following the procedure as described above for complex 3 using 186 mg [Ru(bpy)$_2$Cl$_2$]·2H$_2$O and 119 mg of 8. Yield: 249 mg (81%). UV–vis (MeOH) $\lambda_{max}(\varepsilon)$ = 396 nm (7100) S-bonded, 350 nm (9100) and 495 nm (9100) O-bonded. $E^{\circ\prime}$ Ru$^{3+/2+}$ vs. Ag/Ag$^+$ = 0.92 V S-bonded, 0.53 V O-bonded. ^{1}H NMR (d^6-acetone, 500 MHz) δ: 9.52 (d, 1 H), 9.05 (d, 1 H), 8.90 (d, 1 H), 8.72 (t, 2 H), 8.65 (d, 1 H), 8.58 (t, 1 H), 8.27 (t, 1 H), 8.18 (m, 3 H), 8.15 (t, 1 H), 7.94 (d, 1 H), 7.67 (m, 2 H), 7.59 (t, 1 H), 7.50 (m, 2 H), 7.41 (t, 1 H), 7.32 (d, 1 H), 7.13 (d, 2 H), 6.70 (d, 2 H), 4.32 (d, 1 H), 4.03 (d, 1 H). Elemental Analysis: Calculated for [Ru(C$_{10}$H$_8$N$_2$)$_2$(C$_{14}$H$_{10}$O$_3$SCl)]PF$_6$·0.75H$_2$O: Calculated: C: 47.17%, H: 3.21%, O: 6.93%, N: 6.47%. Found: C: 46.85%, H: 3.44%, O: 6.60%, N: 6.54%.

2.8. Synthesis of [Ru(bpy)$_2$(OSO-BnF)](PF$_6$)·0.5H$_2$O

2-(4-Fluoro-benzylsulfanyl)-benzoic acid, OSBnF (10). 10 was prepared following the procedure as described above for complex 1 starting with 151 mg of thiosalicylic acid and 121 μL of 4-fluorobenzyl bromide. Yield: 149 mg (58%). ^{1}H NMR (d^6-acetone, 300 MHz) δ: 8.01 (d, 1 H), 7.50 (dd, 4 H), 7.24 (m, 1 H), 7.10 (t, 2 H), 4.23 (s, 2 H).

2-(4-Fluoro-benzylsulfinyl)-benzoic acid, OSOBnF (11). 11 was prepared following the procedure as described above for complex 2 starting with 125 mg of complex 10. Yield: 70 mg (53%). ^{1}H NMR (d^6-acetone, 300 MHz) δ: 8.19 (d, 1 H), 7.81 (d, 1 H), 7.73 (t, 1 H), 7.63 (t, 1 H), 7.19 (m, 2 H), 7.02 (m, 2 H), 4.43 (d, 1 H), 3.89 (d, 1 H).

[Ru(bpy)$_2$(OSOBnF)](PF$_6$)·0.5H$_2$O (12). 12 was prepared following the procedure as described above for complex 3 using 102 mg [Ru(bpy)$_2$Cl$_2$]·2H$_2$O and 60 mg of 11. Yield: 104 mg (76%). UV–vis (MeOH) $\lambda_{max}(\varepsilon)$ = 398 nm (6500) S-bonded, 350 nm (8300) and 496 nm (8400) O-bonded. $E^{\circ\prime}$ Ru$^{3+/2+}$ vs. Ag/Ag$^+$ = 0.90 V S-bonded, 0.54 V O-bonded. ^{1}H NMR (d^6-acetone, 500 MHz) δ: 9.53 (d, 1 H), 9.00 (d, 1 H), 8.90 (d, 1 H), 8.69 (d, 2 H), 8.60 (d, 1 H), 8.55 (t, 1 H), 8.25 (t, 1 H), 8.15 (m, 3 H), 8.11 (t, 1 H), 7.90 (d, 1 H), 7.63 (m, 2 H), 7.50 (m, 3 H), 7.39 (t, 1 H), 7.25, (d, 1 H), 6.87 (t, 2 H), 6.70 (t, 2 H), 4.30 (d, 1 H), 4.11 (d, 1 H). Elemental Analysis: Calculated for [Ru(C$_{10}$H$_8$N$_2$)$_2$(C$_{14}$H$_{10}$O$_3$SF)]PF$_6$·0.5H$_2$O: Calculated: C: 48.34%, H: 3.23%, O: 6.63%, N: 6.63%, S: 3.80%. Found: C: 48.42%, H: 3.09%, O: 6.31%, N: 6.57%, S: 3.73%.

2.9. Synthesis of [Ru(bpy)$_2$(OSO-BnOCH$_3$)](PF$_6$)·0.75H$_2$O

2-(4-Methoxy-benzylsulfanyl)-benzoic acid, OSBnOCH$_3$ (13). 13 was prepared following the procedure as described above for complex 1 using 435 mg thiosalicylic acid and 490 μL of 4-methoxybenzyl bromide. Yield: 620 mg (80%). ^{1}H NMR (d^6-acetone, 300 MHz) δ: 8.00 (d, 1 H), 7.50 (m, 2 H), 7.38 (d, 2 H), 7.22 (t, 1 H), 6.89 (d, 2 H), 4.17 (s, 2 H), 3.78 (s, 3 H).

2-(4-Methoxy-benzylsulfinyl)-benzoic acid, OSOBnOCH$_3$ (14). 14 was prepared following the procedure as described above for complex 2 starting with 124 mg of 13. Yield: 114 mg (87%). ^{1}H NMR (d^6-acetone, 300 MHz) δ: 8.18 (d, 1 H), 7.89 (d, 1 H), 7.74 (t, 1 H), 7.63 (t, 1 H), 7.14 (d, 2 H), 6.83 (d, 2 H), 4.40 (d, 1 H), 3.76 (d, 4 H).

[Ru(bpy)$_2$(OSOBnOCH$_3$)](PF$_6$)·0.75H$_2$O (15). 15 was prepared following the procedure as described above for complex 3 using 97 mg [Ru(bpy)$_2$Cl$_2$]·2H$_2$O and 62 mg of 14. Yield: 152 mg (94%). UV–vis (MeOH) $\lambda_{max}(\varepsilon)$ = 402 nm (7100) S-bonded, 350 nm (8600) and 495 nm (8600) O-bonded. $E^{\circ\prime}$ Ru$^{3+/2+}$ vs. Ag/Ag$^+$ = 0.89 V S-bonded, 0.53 V O-bonded. ^{1}H NMR (d^6-acetone, 500 MHz) δ: 9.52 (d, 1 H), 9.02 (d, 1 H), 8.89 (d, 1 H), 8.68 (t, 2 H), 8.62 (d, 1 H), 8.53 (t, 1 H), 8.24 (t, 1 H), 8.15 (m, 3 H), 8.08 (t, 1 H), 7.97 (d, 1 H), 7.63 (m, 2 H), 7.50 (m, 3 H), 7.40 (t, 1 H), 7.31 (d, 1 H), 6.56 (m, 4 H), 4.21 (d, 1 H), 3.90 (d, 1 H), 3.71 (s, 3 H). Elemental Analysis: Calculated for [Ru(C$_{10}$H$_8$N$_2$)$_2$(C$_{15}$H$_{13}$O$_4$S)]PF$_6$·0.75H$_2$O: Calculated: C: 48.80%, H: 3.58%, O: 8.82%, N: 6.51%. Found: C: 48.58%, H: 3.43%, O: 8.54%, N: 6.46%.

2.10. Synthesis of [Ru(bpy)$_2$(OSO-BnNO$_2$)](PF$_6$)·0.75H$_2$O

2-(4-Nitro-benzylsulfanyl)-benzoic acid, OSBnNO$_2$ (16). 16 was prepared following the procedure as described above for complex 1 using 200 mg thiosalicylic acid and 280 mg of 4-nitrobenzyl bromide. Yield: 298 mg (78%). ^{1}H NMR (d^6-acetone, 300 MHz) δ: 8.21 (d, 2 H), 8.01 (d, 1 H), 7.77 (d, 2 H), 7.49 (m, 2 H), 7.25 (m, 1 H), 4.40 (s, 2 H).

2-(4-Nitro-benzylsulfinyl)-benzoic acid, OSOBnNO$_2$ (17). 17 was prepared following the procedure as described above for complex 2 starting with 148 mg of 16. Yield: 144 mg (92%). ^{1}H NMR (d^6-acetone, 300 MHz) δ: 8.20 (d, 1 H), 8.12 (d, 2 H), 7.60-7.73 (m, 3 H), 7.38 (d, 2 H), 4.59 (d, 1 H), 4.14 (d, 1 H).

[Ru(bpy)$_2$(OSOBnNO$_2$)](PF$_6$)·0.75H$_2$O (18). 18 was prepared following the procedure as described above for complex 3 starting with 101 mg [Ru(bpy)$_2$Cl$_2$]·2H$_2$O and 65 mg of 17. Yield: 90 mg (53%). UV–vis (MeOH) $\lambda_{max}(\varepsilon)$ = 391 nm (7400) S-bonded, 345 nm (9500) and 496 nm (8900) O-bonded. $E^{\circ\prime}$ Ru$^{3+/2+}$ vs. Ag/Ag$^+$ = 0.94 V S-bonded, 0.53 V O-bonded. ^{1}H NMR (d^6-acetone, 500 MHz) δ: 9.52 (d, 1 H), 9.00 (d, 1 H), 8.92 (d, 1 H), 8.73 (t, 2 H), 8.68 (d, 1 H), 8.56 (t, 1 H), 8.28 (t, 1 H), 8.15 (m, 4 H), 8.00 (m, 3 H), 7.68 (m, 2 H), 7.60 (t, 1 H), 7.53 (t, 1 H), 7.48 (m, 2 H), 7.34 (d, 1 H), 6.97 (d, 2 H), 4.54 (d, 1 H), 4.25 (d, 1 H). Elemental Analysis: Calculated for [Ru(C$_{10}$H$_8$N$_2$)$_2$(C$_{14}$H$_{10}$O$_5$SN)]PF$_6$·0.75H$_2$O: Calculated: C: 46.60%, H: 3.17%, O: 10.50%, N: 7.99%. Found: C: 46.33%, H: 3.03%, O: 10.23%, N: 8.06%.

3. Results and discussion

Shown in Table 1 are selected data obtained from the study of these compounds and the Hammett parameters for each of the R groups specified in Scheme 1. We have chosen to employ the substituent parameters determined from the ionization of benzoic acid [31]. The ^{1}H NMR spectrum reveals resonances ascribed to the bipyridine and phenyl aromatic ring protons as well as the diastereotopic methylene protons, explicitly depicted in Scheme 1. This latter resonance is responsive to the identity of the R group. Electron-withdrawing groups (NO$_2$, CF$_3$, Cl and F) shift this resonance downfield relative to electron-donating groups (OCH$_3$, CH$_3$

Table 1
R group, Hammett parameter (σ_p), chemical shift (δ; ppm), absorption maxima (λ; nm), Reduction Potentials ($E^{\circ\prime}$; V), and isomerization quantum yield ($\Phi_{S\rightarrow O}$) for [Ru(bpy)$_2$(OSOBnR)]$^+$.

R	σ_p	δ	λ^S_{max}	λ^O_{max}	$E^{\circ\prime}_S$	$E^{\circ\prime}_O$	$\Phi_{S\rightarrow O}$
NO$_2$	0.78	4.40	391	496	0.94	0.53	0.34 ± 0.05
CF$_3$	0.54	4.33	392	496	0.93	0.53	0.13 ± 0.01
Cl	0.23	4.18	396	495	0.92	0.53	0.16 ± 0.01
F	0.06	4.16	398	496	0.90	0.54	0.17 ± 0.01
H	0	4.13	396	496	0.90	0.53	0.22 ± 0.02
CH$_3$	−0.17	4.10	399	496	0.89	0.52	0.13 ± 0.01
OCH$_3$	−0.27	4.06	402	495	0.89	0.53	0.15 ± 0.01

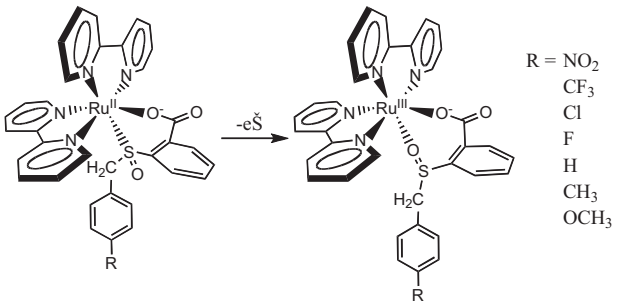

Scheme 1. Compounds employed and reaction investigated in this study.

and H). The ^{1}H NMR and elemental analyses of each of the compounds are consistent with the respective chemical formulae.

Shown in Fig. 1 is the molecular structure of $[Ru(bpy)_2(OSOBnNO_2)]^+$ with selected crystallographic data presented in Table 2. The Ru–N bond distances range from 2.047(3) to 2.087(3) Å and are typical of ruthenium bipyridine distances [32]. The Ru–S and S–O bond distances are 2.208(1) and 1.478(2) Å, respectively. The S–O bond distance is in accord with a great number of ruthenium sulfoxide complexes and is significantly shorter than that observed for uncoordinated dimethylsulfoxide (1.513(5) Å) [33–36]. Similarly, the Ru–S bond distance is consistent with a number of ruthenium sulfoxide structures [20,33,34]. In addition, the structure shows an apparent π-stacking interaction between the benzyl ring and the neighboring bipyridine ring. Indeed, the centroid-to-centroid distance for these two rings is ~3.43 Å.

The visible absorption spectrum of each of these complexes is dominated by a moderately intense ($\varepsilon \sim 10^3\ M^{-1}\ cm^{-1}$) Ru $d\pi \rightarrow$ bpy π^* Metal-to-Ligand Charge-Transfer (MLCT) transition. Sufficient data now exists to suggest that the promoting orbital (Ru $d\pi$) has significant sulfur character [37–39]. Table 1 shows that the S-bonded absorption maxima (λ^S_{max}) are responsive to the identity of R. This change in the MLCT absorption maximum affirms our assertion that the promoting orbital contains some sulfur character [39]. It is not surprising that there are deviations from this trend as absorption maxima represent the difference in energy between excited- and ground-state surfaces.

In accord with similar compounds, [17] these complexes feature photochromic behavior associated with phototriggered S → O isomerization of the bound sulfoxide. Visible irradiation of the ground state S-isomer yields the corresponding ground state O-isomer. Table 1 shows that the MLCT absorption maxima for the O-bonded isomers (λ^O_{max}) are largely invariant with changes in R. Thus, we conclude that the R group has little effect on the ruthenium $d\pi$ HOMO when the sulfoxide is O-bonded. This conclusion necessitates a significant change in orbital overlap between Ru–$S_{sulfoxide}$ and Ru–$O_{sulfoxide}$ groups.

Cyclic voltammograms of these complexes are consistent with electron-transfer triggered S → O isomerization of the sulfoxide (see Supplementary Data) [13,14,16]. The reaction is depicted as one-step in Scheme 1. Shown in Fig. 2 is a representative voltammogram for $[Ru(bpy)_2(OSOBnF)]^+$. The first scan features a one-electron oxidation near +0.95 V vs. Ag/Ag^+. The cathodic scan reveals a quasi-reversible wave assigned to the $Ru^{3+/2+}$ S-bonded

Table 2
Crystal data and structure refinement for $[Ru(bpy)_2(OSOBnNO_2)](PF_6)$.

Identification code	Ru-NO_2
Empirical formula	$C_{35}H_{30}F_6N_5O_6PRuS$
Formula weight	894.74
Temperature	100(2) K
Wavelength	0.71073 Å
Crystal system	Triclinic
Space group	P-1
Unit cell dimensions	a = 10.229(4) Å α = 61.608(5)°
	b = 13.785(5) Å β = 86.977(6)°
	c = 14.072(5) Å γ = 88.524(6)°
Volume	1743.1(11) Å^3
Z	2
Density (calculated)	1.705 Mg/m^3
Absorption coefficient	0.643 mm^{-1}
F(0 0 0)	904
Crystal size	0.17 mm × 0.11 mm × 0.09 mm
Theta range for data collection	1.65–27.00–
Index ranges	−13 <= h <= 12, −17 <= k <= 17, −17 <= l <= 17
Reflections collected	14473
Independent reflections	7458 [R(int) = 0.0412]
Completeness to theta = 27.00$^-$	98.1%
Absorption correction	SADABS
Max. and min. transmission	0.9444 and 0.8985
Refinement method	Full-matrix least-squares on F^2
Data/restraints/parameters	7458/0/552
Goodness-of-fit on F^2	0.941
Final R indices [I > 2sigma(I)]	R1 = 0.0442, wR2 = 0.0941
R indices (all data)	R1 = 0.0611, wR2 = 0.0966
Largest diff. peak and hole	0.813 and −1.469e^{-3}

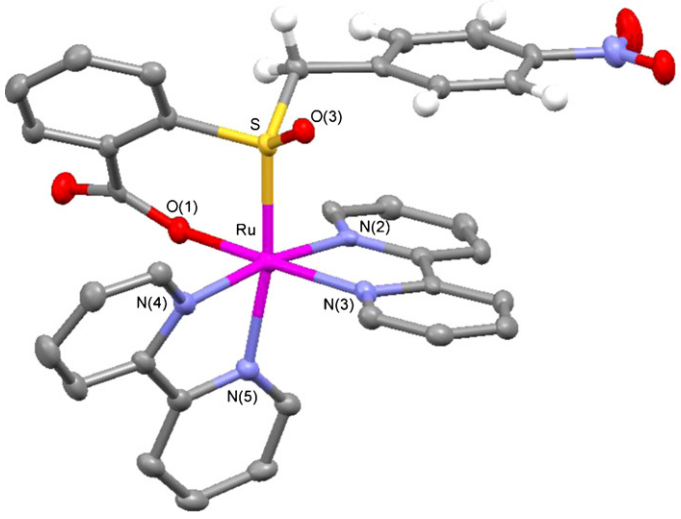

Fig. 1. Molecular structure of $[Ru(bpy)_2(OSOBnNO_2)]^+$. Atoms are thermal ellipsoids rendered at 50% probability. Hydrogen atoms have been omitted for clarity.

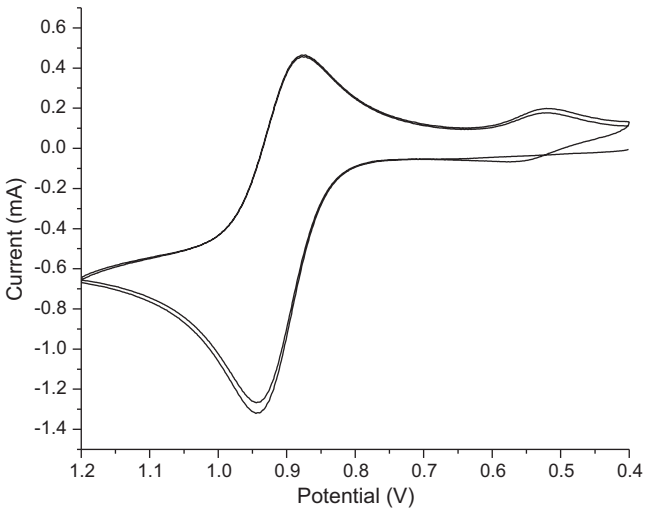

Fig. 2. Cyclic voltammogram of $[Ru(bpy)_2(OSOBnF)]^+$. Scan rate 0.1 V/s, WE:platinum, CE:platinum, RE:$Ag/AgPF_6$).

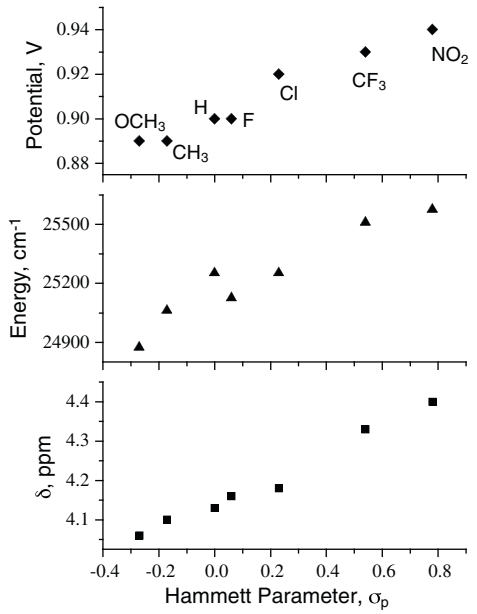

Fig. 3. Plot of $E_S^{\circ'}$ (top, ♦), S-bonded absorption energy (E_{max}^S, ▲, middle), and chemical shift (δ, ■, bottom) of diastereotopic methylene protons vs. the Hammett parameter σ_p. The identity of the R group is denoted in the top plot.

couple ($E_S^{\circ'}$). Scanning to less positive potentials reveals another couple assigned to the $Ru^{3+/2+}$ O-bonded isomer ($E_O^{\circ'}$). Just as oxidation triggers S → O isomerization, reduction of Ru^{3+} to yield Ru^{2+} prompts O → S isomerization. The $Ru^{3+/2+}$ O-bonded couple is only observed following oxidation of the more positive couple. The appearance of the voltammogram is dependent upon the isomerization rates, the switching potentials and the scan rate.

Shown in Table 1 are $E_S^{\circ'}$ and $E_O^{\circ'}$ values for isomers of $[Ru(bpy)_2(OSO\text{-}BnR)]^+$. The data show that $E_O^{\circ'}$ values are invariant with changes in the R group. In contrast, $E_S^{\circ'}$ decreases by nearly 50 mV as the R group becomes more electron-donating. Such shifts are not uncommon in electrochemical studies of ruthenium complexes [40]. For example, in studies of $[(H_3N)_5Ru(L)]^{2+}$, where L is a 4-substituted pyridine, the $Ru^{3+/2+}$ reduction potential varies predictably based on the π-accepting ability of pyridine (py). For $[(H_3N)_5Ru(py)]^{2+}$, this couple is +0.30 V vs. NHE, which shifts to +0.322 V, +0.375 V, and +0.394 V for *p*-Cl-pyridine, *p*-$CONH_2$-pyridine (isonicotinamide) and *p*-CF_3-pyridine, respectively [41–43]. However, these shifts are due to alterations of ligand acceptor orbitals involved in bonding to ruthenium. The π* orbitals on pyridine stabilize the Ru dπ orbital set altering $E^{\circ'}$ accordingly. In the present study, shifts in $E_S^{\circ'}$ are due to modifications of the benzyl group bound to the sulfoxide. There is no apparent direct orbital interaction between the distant R-group and ruthenium.

The voltammetric results are in accord with both the absorption and chemical shift data and further illustrate that the R group affects the basicity of the sulfoxide group when sulfur is bound to ruthenium, but not when oxygen is bound to ruthenium. The R group influences the chemical shift of the methylene protons, the absorption maxima of the lowest energy visible transition and the $Ru^{3+/2+}$ reduction potential. Indeed, plots of the methylene chemical shift (δ, ppm), the charge-transfer absorption maxima (E_{max}^S, cm^{-1}), or the S-bonded reduction potential ($E_S^{\circ'}$, V) vs. σ_p are linear, indicating that the identity of R effects these bonding and metal-based properties in a linear fashion (Fig. 3).

Quantum yields of S → O isomerization ($\Phi_{S\rightarrow O}$) were collected to determine if a correlation between the identity of the R group and the excited state rates of isomerization could be identified. Shown in Table 1 are the $\Phi_{S\rightarrow O}$ values found for each compound listed as a function of R group. It is evident that the greatest and smallest values are found for the NO_2 and OCH_3 substituted complexes, respectively. However, the complexes between these two extremes do not reveal a monotonic or linear correlation. Thus, while the R group affects metal-based properties (absorption maxima and reduction potential), it does not appear to effect isomerization quantum yields in accord with a linear free energy relationship.

While speculative, a possible explanation for the lack of a linear free energy relationship is that the isomerization mechanism has changed significantly within these complexes. Such a change may involve stabilization of the transition state to form an intermediate or involve a dramatic shifting of the transition state along the reaction coordinate. The obvious transition state for this reaction is an η^2-bound sulfoxide. At present, we are not aware of any mononuclear η^2-bound sulfoxide ligands, but there are three binuclear structures featuring an unusual, Ru–S–O–Ru bridging mode from dimethylsulfoxide [44–46] as well as a metastable η^2-bound SO_2-ruthenium complex formed from irradiation of the S-bonded complex [47,48].

4. Conclusions

We have prepared a family of ruthenium sulfoxide complexes that differ only in the presence of tunable R group on the benzyl ligand. The data show that the chemical shift of the methylene linkage (δ_{CH2}), the S-bonded $Ru^{3+/2+}$ reduction potential ($E_S^{\circ'}$), and the S-bonded MLCT absorption maximum (λ_{max}^S) all change predictably with the identity of R. We do not observe a predictable effect between the identity of R and $\Phi_{S\rightarrow O}$. Future work will involve the design of a new family of complexes in which the tunable R group may be placed directly on or closer to the sulfoxide. In addition, excited state rates of isomerization in these complexes will be measured directly and compared to determine if a linear free energy relationship exists for these compounds.

Acknowledgements

We are grateful to Melanie Heying and Shadrick Paris for helpful discussions. JJR thanks NSF (CHE 0809669), Ohio University, Condensed Matter and Surface Science (CMSS) and the NanoBioTechnology Initiative (NBTI) for funding of this work. BLP thanks OU for a Provost's Undergraduate Research Fund (PURF) award and the Manasseh-Cutler Scholar Program. BAM recognizes NDSEG for a fellowship.

Appendix A. Supplementary data

Supplementary data associated with this article can be found, in the online version, at doi:10.1016/j.jphotochem.2010.11.002.

References

[1] V. Balzani, A. Credi, B. Ferrer, S. Silvi, M. Venturi, Top. Curr. Chem. 262 (2005) 1.
[2] J.-P. Collin, V. Heitz, J.-P. Sauvage, Top. Curr. Chem. 262 (2005) 29.
[3] N.N.P. Moonen, A.H. Flood, J.M. Fernandez, J.F. Stoddart, Top. Curr. Chem. 262 (2005) 99.
[4] I. Aprahamian, J.-C. Olsen, A. Trabolsi, J.F. Stoddart, Chem. Eur. J. 14 (2008) 3889.
[5] Y.-L. Zhao, W.R. Dichtel, A. Trabolsi, S. Saha, I. Aprahamian, J.F. Stoddart, J. Am. Chem. Soc. 130 (2008) 11294.
[6] K.A. McNitt, K. Parimal, A.I. Share, A.C. Fahrenbach, E.H. Witlicki, M. Pink, D.K. Bediako, C.L. Plaisier, N. Le, L.P. Heeringa, D.A. Vander Griend, A.H. Flood, J. Am. Chem. Soc. 131 (2009) 1305.
[7] C.J. Adams, K.M. Anderson, N.G. Connelly, E. Llamas-Rey, A.G. Orpen, R.L. Paul, Dalton Trans. (2007) 3609.
[8] T. Hamaguchi, Y. Inoue, K. Ujimoto, I. Ando, Polyhedron 27 (2008) 2031.
[9] T. Hamaguchi, K. Ujimoto, I. Ando, Inorg. Chem. 46 (2007) 10455.
[10] O. Johansson, R. Lomoth, Chem. Commun. (2005) 1578.
[11] O. Johansson, R. Lomoth, Inorg. Chem. 47 (2008) 5531.
[12] S.A. Angell, C.W. Rogers, Y. Zhang, M.O. Wolf, W.E. Jones Jr., Coord. Chem. Rev. 250 (2006) 1829.

[13] M. Sano, Struct. Bond. 99 (2001) 117.
[14] M. Sano, H. Taube, Inorg. Chem. 33 (1994) 705.
[15] M.K. Smith, J.A. Gibson, C.G. Young, J.A. Broomhead, P.C. Junk, F.R. Keene, Eur. J. Inorg. Chem. (2000) 1365.
[16] A. Yeh, N. Scott, H. Taube, Inorg. Chem. 21 (1982) 2542.
[17] J.D.P. Butcher, A.A. Rachford, J.L. Petersen, J.J. Rack, Inorg. Chem. 45 (2006) 9178.
[18] N.V. Mockus, S. Marquard, J.J. Rack, J. Photochem. Photobiol. A 200 (2008) 39.
[19] N.V. Mockus, D. Rabinovich, J.L. Petersen, J.J. Rack, Angew. Chem. Int. Ed. 47 (2008) 1458.
[20] A.A. Rachford, J.L. Petersen, J.J. Rack, Inorg. Chem. 44 (2005) 8065.
[21] A.A. Rachford, J.L. Petersen, J.J. Rack, Inorg. Chem. 45 (2006) 5953.
[22] A.A. Rachford, J.L. Petersen, J.J. Rack, Dalton Trans. (2007) 3245.
[23] A.A. Rachford, J.J. Rack, J. Am. Chem. Soc. 128 (2006) 14318.
[24] J.J. Rack, N.V. Mockus, Inorg. Chem. 42 (2003) 5792.
[25] J.J. Rack, A.A. Rachford, A.M. Shelker, Inorg. Chem. 42 (2003) 7357.
[26] J.J. Rack, J.R. Winkler, H.B. Gray, J. Am. Chem. Soc. 123 (2001) 2432.
[27] B.P. Sullivan, D.J. Salmon, T.J. Meyer, Inorg. Chem. 17 (1978) 3334.
[28] B.A. McClure, E.R. Abrams, J.J. Rack, J. Am. Chem. Soc. 132 (2010) 5428.
[29] J.G. Calvert, J.N. Pitts, Photochemistry, Wiley, New York, 1966.
[30] G.M. Sheldrick, SHELXTL, Crystallographic Software Package, Version 6.10, Bruker-AXS ed, Madison, WI, 2000.
[31] C.D. Ritchie, W.F. Sager, Prog. Phys. Org. Chem. 2 (1964) 323.
[32] D.P. Rillema, D.S. Jones, H.A. Levy, Chem. Commun. (1979) 849.
[33] M. Calligaris, Coord. Chem. Rev. 248 (2004) 351.
[34] M. Calligaris, O. Carugo, Coord. Chem. Rev. 153 (1996) 83.
[35] F.C. March, G. Ferguson, Can. J. Chem. 49 (1971) 3590.
[36] R. Thomas, C.B. Shoemaker, K. Eriks, Acta Cryst. 21 (1966) 12.
[37] B.A. McClure, N.V. Mockus, D.P. Butcher Jr, D.A. Lutterman, C. Turro, J.L. Petersen, J.J. Rack, Inorg. Chem. 48 (2009) 8084.
[38] I. Ciofini, C.A. Daul, C. Adamo, J. Phys. Chem. A 107 (2003) 11182.
[39] D.A. Lutterman, A.A. Rachford, J.J. Rack, C. Turro, J. Phys. Chem. A 113 (2009) 11002.
[40] A.B.P. Lever, Inorg. Chem. 29 (1990) 1271.
[41] H.S. Lim, D.J. Barclay, F.C. Anson, Inorg. Chem. 11 (1972) 1460.
[42] J.A. Marchant, T. Matsubara, P.C. Ford, Inorg. Chem. 16 (1977) 2160.
[43] T. Matsubara, P.C. Ford, Inorg. Chem. 15 (1976) 1107.
[44] S. Geremia, S. Mestroni, M. Calligaris, E. Alessio, Dalton Trans. (1998) 2447.
[45] S.F. Lessing, S. Lotz, H.M. Roos, P.H. van Rooyen, Dalton Trans. (1999) 1499.
[46] T. Tanase, T. Aiko, Y. Yamamoto, Chem. Commun. (1996) 2341.
[47] A.Y. Kovalevsky, K.A. Bagley, J.M. Cole, P. Coppens, Inorg. Chem. 42 (2003) 140.
[48] A.Y. Kovalevsky, K.A. Bagley, P. Coppens, J. Am. Chem. Soc. 124 (2002) 9241.